

1 The weather of 1740, the coldest year in Central Europe in 600 years

2

3 Stefan Brönnimann^{1,2,*}, Janusz Filipiak³, Siyu Chen^{1,2}, and Lucas Pfister^{1,2}

4 ¹*Oeschger Centre for Climate Change Research, University of Bern, Bern, Switzerland*

5 ²*Institute of Geography, University of Bern, Bern, Switzerland*

6 ³*Department of Physical Oceanography and Climate Research, University of Gdansk, Gdansk, Poland*

7

8 *corresponding author: Stefan Brönnimann, stefan.broennimann@giub.unibe.ch

9

10

11 Abstract

12 The winter 1739/40 is known as one of the coldest winters in Europe since early instrumental measurements
13 began. Many contemporary sources discuss the cold waves and compare the winter to that of 1708/09. It is less
14 well known that the year 1740 remained cold until August and again in October, and that negative temperature
15 anomalies are also found over Eurasia and North America. The 1739/40 cold season over northern midlatitude
16 land areas was perhaps the coldest in 300 years, and 1740 was the coldest year in Central Europe in 600 years.
17 New monthly, global climate reconstructions allow addressing this momentous event in greater detail, while
18 daily observations and weather reconstructions give insight into the synoptic situations. Over Europe, we find
19 that the event was initiated by a strong Scandinavian blocking in early January, allowing the advection
20 continental cold air. From February until June, high pressure dominated over Ireland, arguably associated with
21 frequent East Atlantic blocking. This led to cold air advection from the cold northern North Atlantic. During the
22 summer, cyclonic weather dominated over Central Europe, associated with cold and wet air from the Atlantic.
23 The possible role of oceanic influences (El Niño) and external forcings (eruption of Mount Tarumae in 1739)
24 are discussed. While a possible El Niño event might have contributed to the winter cold spells, the East Atlantic
25 blocking is arguably unrelated to either El Niño or the volcanic eruption. In all, the cold year of 1740 marks one
26 of the strongest, arguably unforced excursions in European temperature.

27

28 Introduction

29 The winter 1739/40 is known as an extremely cold winter in Central Europe, rivalling the winter of
30 1708/09 as the coldest in the past several hundred years. The winter was severe across Europe,
31 including Switzerland (Pfister and Wanner, 2021), Poland (Filipiak et al., 2019), the British Isles
32 (Manley, 1957; Lamb 1967, [Jones and Briffa, 2006](#)), Netherlands, and Germany ([Jones and Briffa, 2006](#))
33 and other regions. The winter started early, already in October 1739 and ended only in June
34 1740, and it is particularly well known for frozen rivers and ice floods. [In London, a frost fair was](#)
35 [held on River Thames and in Ireland River Shannon froze \(Dickson, 1997; see Mateus \(2021\) for an](#)
36 [overview of early instrumental data in Ireland\). In Italy the lagoon of Venice froze \(Camuffo, 1987\).](#)
37 Filipiak et al. (2019) reported that after unusually cold easterly winds in mid-October 1739 at the
38 coast of the Baltic Sea, there were very heavy snowfalls and several waves of severe frost in

39 November 1739, January 1740 and again in February and March, with the most extreme conditions in
40 January 1740. The coastal waters of the Baltic Sea and particularly the Vistula River were frozen until
41 mid-April with the ice thickness exceeding 50 cm. Water from the huge amounts of snow melting in
42 April caused a large and long-lasting flood in the Baltic lowlands. In Ireland, the intense cold lasted
43 for weeks, interspersed with only short break of slight thaw (Gillespie, 1939). Potatoes and turnips
44 were destroyed, cattle and even fish died (Dickson, 1997). Among the consequences was the Irish
45 famine of 1740/41 (Engler et al., 2013) [triggering substantial migration](#). However, the winter was
46 only the start of a series of adverse weather and climate events, which led to high mortality and high
47 cereal prices also in Central Europe (Post, 1984). Due to the frozen rivers and long-term shutdown of
48 mills in Poland there was even a shortage of bread, and the administrative authorities of many cities
49 started to provide food, wood and means of subsistence to the poorest people (Filipiak et al. 2019).
50 Jones and Briffa (2006) pointed out that the entire year 1740 was cold and that it particularly
51 contrasted with the warm 1730s. [The annual average Central England Temperature was above the
52 1961-1990 average in all years from 1730 to 1738 \(Manley, 1974, Parker et al., 1992\).](#)

53 Reconstructions of sea-level pressure have allowed characterising the anomalies atmospheric
54 circulation of this specific period in a bit more detail. Jones and Briffa (2006), using hand analysed
55 monthly sea-level pressure fields, noted that in winter, the Icelandic Low and the Azores High were
56 weaker than normal and the dominant feature was a continental or Scandinavian High. Engel et al.
57 (2013), using sea-level pressure and 500 hPa geopotential height reconstruction of Luterbacher et al.
58 (2002), additionally found a strong high-pressure situation in spring 1740, resembling a negative
59 phase of the East Atlantic pattern and leading to cold air advection from the northwest.

60 It is less well known, however, that the winter 1739/40 was not only cold in Europe but also in North
61 America and parts of Asia. A cold season (Oct-May) temperature field reconstruction for midlatitude
62 (35-70° N) land areas from 1701-2020 indicates that this might have been the coldest cold season of
63 the last 300 years (Reichen et al. 2022). Recently, a comprehensive, global 3-dimensional climate
64 reconstruction was published (Valler et al., 2024) and numerous additional meteorological time series
65 have been digitised such that we can now study this event in more detail and on the daily scale, i.e.,
66 the scale of the weather events.

67 Here we study the weather of the year of 1740 using the new reconstructions combined with daily
68 meteorological series. We analyse sequence of events on monthly scale, zoom into prominent cold air
69 outbreaks on daily scale, and analyse role of forcings and large-scale circulation mechanisms.

70

71 **Data and Methods**

72 *Reconstructions*

73 We use the ModE-RA (Modern Era Reanalysis) family of reconstructions (Valler et al., 2024), which
74 provide monthly, global 3-dimensional fields back to 1421. Similar as the precursor product
75 EKF400v2 (Valler et al., 2022), ModE-RA is based on the offline assimilation of a large amount of
76 natural proxies, documentary data, and instrumental observations into an ensemble of 20 atmospheric
77 model simulations (ModE-Sim, Hand et al., 2023). Another product, termed ModE-RAclim, was
78 generated by assimilating the same observations into a sample of 100 realisations, randomly drawn
79 from all members and all model years of ModE-Sim. Analysing ModE-Sim and ModE-RAclim along
80 with ModE-RA allows ~~to~~ disentangling the role of forcings and observations. ModE-Sim was forced
81 by monthly sea-surface temperatures (Samakinwa et al., 2021, Titchner and Rayner, 2014), volcanic,
82 land-surface and solar forcings following the PMIP4 protocol (Jungclaus et al., 2017). It does not see
83 the assimilated observations but only the model boundary conditions. In contrast, ModE-RAclim does
84 not see the time-dependent boundary conditions, but only the observations. We performed the
85 analyses on the individual ensemble members, but when plotting spatial fields we show the ensemble
86 mean only. When plotting anomalies these were expressed relative to the 30 preceding years (1710-
87 39). Note that the ModE-RA data set was constructed as anomalies from a 71-yr moving average,
88 therefore the last three decades of the data set are less well constrained.

89 For comparison, we also used the reconstruction XBRWccc (Reichen et al., 2022), which provides
90 cold season (~~May-Oct~~Oct-May) temperature field reconstructions for the northern extratropics. It is
91 based on a Bayesian reweighting approach of model simulations that are very similar as ModE-Sim.
92 Only phenological data (mostly ice phenology, i.e., the freezing and thawing dates of rivers and lakes,
93 some plant phenological data) are used to constrain this reconstruction.

94 *Meteorological series*

95 In this paper we work with daily meteorological time series from measurements and observations,
96 which were inventoried in Brönnimann et al. (2019) and compiled in Lundstad et al. (2022). These
97 compilations are complemented with additional series. Table 1 gives an overview of the series used
98 and their sources. [Note that there are several additional sources that only provide monthly data. They](#)
99 [are not listed in the Table but are included in the ModE-RA data set. Prominent long monthly](#)
100 [temperature are those from De Bilt, Netherlands, since 1706 or the Central England temperature since](#)
101 [1659 \(but daily only after 1772, Parker et al., 1992\).](#)

102 For some of the analyses, all segments were deseasonalized by fitting and subtracting the first two
103 harmonics of the annual cycle and then standardized. This allows for better comparison of series with
104 different numbers of observations per day and allows including series on unknown scales (such as
105 temperature in Berlin). Note that a unique reference period that works for all series does not exist. If
106 possible we used 1731-50, but several of the segments were too short (in ~~one~~ case slightly longer;
107 following ~~a~~in existing segment). This reference is shorter than that for ModE-RA (analyses of the two
108 data sets are performed separately). For the special case of Montpellier, where we have very irregular

109 data (but which always include the monthly minima and maxima), we proceeded in the same way for
 110 the deseasonalizing. However, because the series consists mostly of maxima and minima, it has a
 111 standard deviation that is ca. 1.5-2 times larger than that at other stations. Therefore, we inflated the
 112 standardized anomalies by 1.5.

113

114 **Table 1.** Locations and sources of daily weather data used in this study, variables (Var., p = pressure, mslp =
 115 mean sea-level pressure (converted by other authors), T = temperature, dir = wind direction, RR = precipitation,
 116 wn = weather notes), period and source

Location	Var.	Period	Source
Haarlem	T	1735-42	KNMI
Leiden	T, p	1740-50	KNMI
London	mslp	1731-50	Cornes et al., 2012, 2023
Montpellier	(T, p)*	1738-48	Lundstad et al., 2022
Paris	T	1732-57	Rousseau 2019
Versailles	wn		Société Météorologique de France, 1866
Berlin	T, p	1738-43	Brönnimann and Brugnara, 2023
Gdansk	T, p, wn	1740	Filipiak et al., 2019
Nuremberg	p, dir	1732-43	Brönnimann and Brugnara, 2023
Uppsala [†]	T, mslp	1731-50	Bergström and Moberg, 2002
Padova	T, mslp, RR	1731-50	Camuffo and Jones 2002, Stefanini et al. 2024
Bologna	T	1731-50	Camuffo and Jones 2002, Camuffo et al., 2017
Channel	dir	1731-50	Barriopedro et al. 2014
St. Blaise	(dir), wn		Pfister et al. 2017

117 * pressure was only used until April 1746, morning (typically 3-8 AM) and afternoon (mostly 3 PM) were treated separately.

118 [†] until 1738 these were presumably indoor measurements (Bergström and Moberg, 2002) that have a reduced diurnal cycle
 119 amplitude and perhaps also day-to-day variability, but only a small bias.

120 In addition to the instrumental series, we also consulted weather diaries and other historical sources to
 121 better characterize the weather of 1740. This includes observations from Gdansk (Filipiak et al.,
 122 2019), Berlin (Brönnimann and Brugnara, 2023), Versailles (Société Météorologique de France,
 123 1866), and St. Blaise (from EURO-CLIMHIST, Pfister et al., 2017). Note that most of these series
 124 were assimilated into ModE-RA.

125 Daily reconstructions of sea-level pressure fields

126 For the analyses of daily weather, we not only used the raw data, but reconstructed daily pressure
 127 fields over Europe from the pressure observations using a simple analog approach (see also Pappert et
 128 al., 2022). For that we used the ERA5 reanalysis (Hersbach et al., 2020) from 1940-2023. We
 129 extracted sea-level pressure at the 1740 observation locations, deseasonalized and standardized the
 130 data in the same way as described above (using the entire period) and then determined, for each day in
 131 1740, the closest analog day in ERA5 within a window of ± 60 calendar days of the target day. We

Formatted: Superscript

Formatted: Superscript

132 used the Euclidian distance as a distance measure. Once the closest analog is found, the sea-level
133 pressure field for that day is taken as the reconstruction, without any further postprocessing.

134 An evaluation was performed by applying the procedure to the year 1940 within ERA5 using 1941-
135 2023 as pool of analogs. Comparing the results against the actual fields in 1940 (Fig. S1) shows
136 excellent correlations and a low root-mean squared error over central Europe, but a rapid deterioration
137 towards the Southwest and Northeast.

138 *Index time series*

139 In addition to spatial analyses and analyses of the instrumental series, we also calculated time series
140 within ModE-RA. We defined Central European temperature as the average 2 m temperature in the
141 region 5-25° E, 45-55° N. The index was also calculated in the CRUTEM5 data set (Osborn et al.,
142 2021) in order to extend the reconstruction to the present. Furthermore, we calculated indices for the
143 North Atlantic Oscillation (NAO), [the Scandinavian Index \(SCAN\)](#), and the East Atlantic Pattern
144 (EA). The former was defined as the sea-level pressure difference between the locations of Lisbon
145 and Gibraltar. [SCAN was defined as the sea-level pressure difference between 15°E/40°N and 30°E](#)
146 [/65°N](#). For the latter, different definitions exist. We use the sea-level pressure difference between 30°
147 E/45° N and 20° W/55° N, which is similar to Barnston and Livezey (1987) and denoted EA1 in the
148 following. We also define an index EA2 as the difference between 30° E/55° N and 20° W/55° N,
149 which is more similar to the definition of Wallace and Gutzler (1981). Note that in all indices, only
150 the difference was calculated and no standardization was used, since the standard deviation in the
151 ModE-RA datasets changes over time. We mostly analyse Jan-Feb for NAO and Mar-May for EA1
152 and EA2.

153 Finally, we also used a NINO3.4 index (Sep-Feb) which we calculated from ModE-RA 2 m
154 temperature data. For addressing the volcanic forcing, we used the estimated radiative forcings for
155 different volcanic eruptions as given in Sigl et al. (2015). We selected eruptions with a global forcing
156 stronger than -2 W m^{-2} . For both NINO3.4 and volcanic years, we analysed the NAO and EA indices
157 of the subsequent winter and spring periods. For NINO3.4 we used a correlation analyses, for
158 volcanic eruptions compositing.

159

160 **Results**

161 *Descriptions of the weather and impacts in Europe*

162 The low temperatures in the winter 1739/40 and the consequences are well documented across
163 Europe. Here we present the weather information from the three locations listed in Table 1
164 ([Versailles](#), [Gdansk](#), and [St. Blaise](#)). Interestingly, the winter 1739/40 was compared with the winter
165 of 1708/09, which was still in the memory of the people at that time, in several of the sources. As an
166 example, Fig. 1 shows an excerpt of a weather diary led by Christine Kirch (Brönnimann and

167 Brugnara, 2023). The text, [spanning-describing](#) a travel from Paris to Luxembourg, speaks of freezing
168 wine, fountains freezing to the ground, and bursting bridges. At several instances it compares
169 measured temperatures with those in 1709 and finds that 1740 temperatures were even lower.

170 Commissaire Narbonne noted the weather in Versailles from 1709-45 (Société Météorologique de
171 France, 1866). According to his notes, the Seine was frozen, and public fires were lit in the streets of
172 Paris from 9 Jan to 9 Feb 1740 and similarly in Versailles. Severe frost is noted in January, February
173 and March. Low temperatures are noted throughout the year. On 7-8 October, during grape harvest,
174 Versailles experienced a severe frost and grapes were frozen.

175 According to two prominent scientists of Gdansk at the Baltic Sea coast, Northern Poland – Michael
176 Christian Hanov (a pioneer of systematic instrumental measurements in the city) and Gottfried Reyger
177 (botanist and chronicler), [the](#) winter of 1740 in Gdansk was unprecedented (Filipiak et al. 2019).
178 Hanov recorded the lowest temperatures between 8th and 14th [January](#), 1740 with a minimum on the
179 morning of the 10th [January](#). Further, extreme cold occurred also between 1st and 7th [February](#), 17th
180 and 25th [February](#) and in a few selected days in March. Reyger compared several severe winters in the
181 18th century (1709, 1729, 1740 and 1784) and pointed out that winter of 1740 was undoubtedly the
182 coldest one, however in 1709 the duration of severe frost was even higher. Harsh weather conditions
183 during winter and a late and cool spring resulted in a very late appearance of vegetation – species
184 usually present in early March were observed only in the last days of April. Although the ice on the
185 Baltic Sea and the Vistula remained longer in April 1771 and 1784 than in 1740, the flood lasting
186 many weeks had a significant impact on the economy in 1740. Both researchers noticed unnatural
187 behaviour of animals and numerous cases of animals freezing, both farm animals and wild ones.
188 Among the increased number of human diseases, many frostbites were noticed, but the mortality rate
189 did not increase noticeably. Further, Hanov pointed out an exceptionally cold May with extremely
190 cloudy conditions (whereas [the](#)-cloudiness is usually minimum in May in the annual course), fog and
191 snow constantly present even at the end of the month, several frosts in June and unusual weather
192 conditions during summer. The harvest, delayed by a cold and wet August, took place in an
193 exceptionally sunny and warm September (according to Reyger it was “the best weather in the whole
194 year”), the autumn fruit harvest was also very good. October was cold again in Gdansk. The first
195 snowfall occurred already on [the](#)-5th[Oct](#). Hanov also reported the anomalously cold weather in
196 selected months of 1740 (particularly in January) in other cities in Europe, i.e., Königsberg, Hamburg,
197 Kiel, Wittenberg, the Hague, Uppsala and Petersburg.

Die Wein ist in dem Keller gefroren. Ich hab
 von einem Kisten, Wein ist gefroren
 gefroren. Die Weinberge sind gefroren und hat auf
 diesem Jahre auf Landbau geblieben sind von dem
 kalten als davor gefallen worden. Das ist ein
 vorigen Monat, Ende in Winter auf 8 Tage, ist man
 ein Pfaffenman, was ich eine ganze Kette andrückt,
 das laufen man auf im Jahr 1709, befristet Jahr. 70
 was ein großer Kist, das von Kisten gegen Kisten ging,
 sind gefroren in Winter. Was ich bei dem Jahr
 ist die Kiste in der Jahre wo dem größten Jahr
 gefroren. Die Weinberge sind auf 3 Pfaffenman Kisten
 das Jahr gewaltigen Kette geblieben. Die Kiste das
 sind 4000 an, ist aber ein 20000 geringere, als die am
 11ten und 12ten gefroren.

Ergebnis vom 11. Jan.

Die Kiste, die wir hier einige Zeit gefüllt ist, ist
 ganz an, das man bei dem Landbau geblieben in
 dem Land nicht gefroren. Die Kisten in dem Land
 von Manich ist die mit dem Kisten gefroren, was ich
 bleibt im Jahr 1704 nicht gefroren worden etc.

198
 199 **Fig. 1.** Excerpt of “Kirch diary” led by Christine Kirch for 13 and 14 January 1740 (see Brönnimann and
 200 Brugnara, 2023).

201 In Switzerland, a detailed weather diary is available from the vine-grower family Péter from St.
 202 Blaise. The diary notes the very low temperature from 8-12 January, which are followed by warmer
 203 weather. However, all of February then was described as “very cold” in St. Blaise. In February and
 204 March, water bodies were frozen and navigation stopped on Lake Biel and Lake Morat, and this
 205 continued into April (19 Apr, parts of Lake Neuchatel were frozen). Most of March the weather diary
 206 notes “frost”. Frost impact on grapevines was reported in April and May. Snowfall was observed until
 207 8 May (at low elevations) and 20 May (at higher elevations).

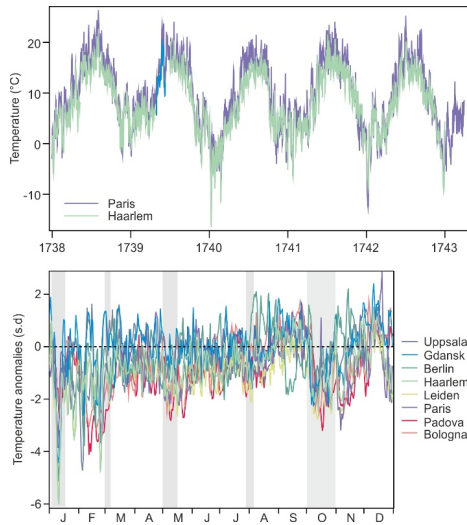
208 *Instrumental measurements*

209 For the year 1740, eight daily temperature series are available, although Montpellier is very sporadic
 210 and Haarlem and Leiden are very close. More series would exist, but are not available in daily,
 211 digitised format (see Brönnimann et al., 2019). As an example, Fig. 2 (top) shows the raw daily mean
 212 temperature series from Paris and Haarlem from 1738-43. The low temperatures in the winter 1739/40
 213 clearly stand out, and it becomes visually apparent that also the other seasons were colder than the
 214 other years shown (the winter 1741/42 also is very cold). The winter 1739/40 began early, with low
 215 temperatures in October and November 1739. After a warm December, temperatures then dropped in
 216 January. Low temperatures lasted consistently until August, and October and November were again
 217 very cold.

218 After deseasonalizing and standardizing the series (Fig. 2, middle), it can be seen that temperatures
 219 were below average (1731-1750, where possible) at most stations during most of the year. Only
 220 August and September had warm intervals. In the following we discuss several episodes (marked with
 221 grey bars) in more detail by analysing the daily series (Fig. 3) and pressure fields (Fig. 4).

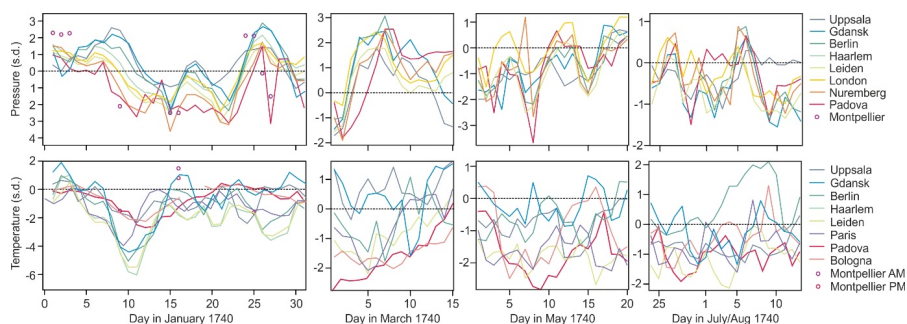
222 One of the most severe cold spells occurred in the first half of Jan 1740. It peaked at 10-11 Jan and
 223 brought very low temperatures to Western Europe, up to 6 standard deviations below the mean, which
 224 is extraordinary (Fig. 3). The cold was not so intense in the North and South, i.e., in Uppsala and
 225 Bologna (although temperature also fell below -2 standard deviations at those locations; [note that in](#)
 226 [Uppsala, part of the reference period is based on indoor data](#)). Temperature remained low also during
 227 the rest of the month, with a similar pattern. Pressure was below normal in the South and above
 228 normal in the North; the gradient in the standardized anomalies persisted during the entire month. The
 229 distinct pressure drop in Padova on 27 Jan is suspect and could be outlier, but also Montpellier shows
 230 a pressure drop.

231 In early March 1740, negative temperature anomalies were observed in the South and West, though
 232 not nearly as strong as in the January case. All stations show a very strong pressure increase from
 233 strong negative anomalies to very high positive anomalies that persisted for 10 days. The third cold
 234 period, in May 1740, was less homogeneous. Again, temperatures were persistently low in Western
 235 Europe (Paris, Leiden), only slightly below normal in Gdansk and Uppsala. Temperatures were also
 236 low in Bologna the beginning of the month and again towards 20 May. Pressure was generally below
 237 normal, but above in London.



238 **Fig. 2.** (top) Daily temperature series from two selected European stations from 1738-43, ([middlebottom](#))
 239 standardised daily temperature anomaly at seven European sites in 1740 [and \(bottom\) the only two available](#)
 240 [non-European temperature series that cover the boreal winter 1739/40](#). Shaded bars in the middle panel denote
 241 the periods chosen for more detailed analysis.

243



244
 245 **Fig. 3.** Standardized temperature and sea-level pressure anomaly series for the four episodes 1-31 Jan, 1-15 Mar,
 246 1-20 May, and 24 Jul to 14 Aug 1740.

247 The fourth chosen episode featured below normal temperature at most stations. An exception is
 248 Berlin, where temperatures exceeded 2 standard deviations. This appears suspicious, but we have no
 249 indications that could lead us to remove the data. Pressure was mostly below normal. Padova and
 250 Uppsala show sometimes a different behaviour whereas all other stations run in parallel. Overall,
 251 analysing the long pressure time series from London or Uppsala, the year 1740 did not feature
 252 particularly many extreme days.

253 *Weather maps*

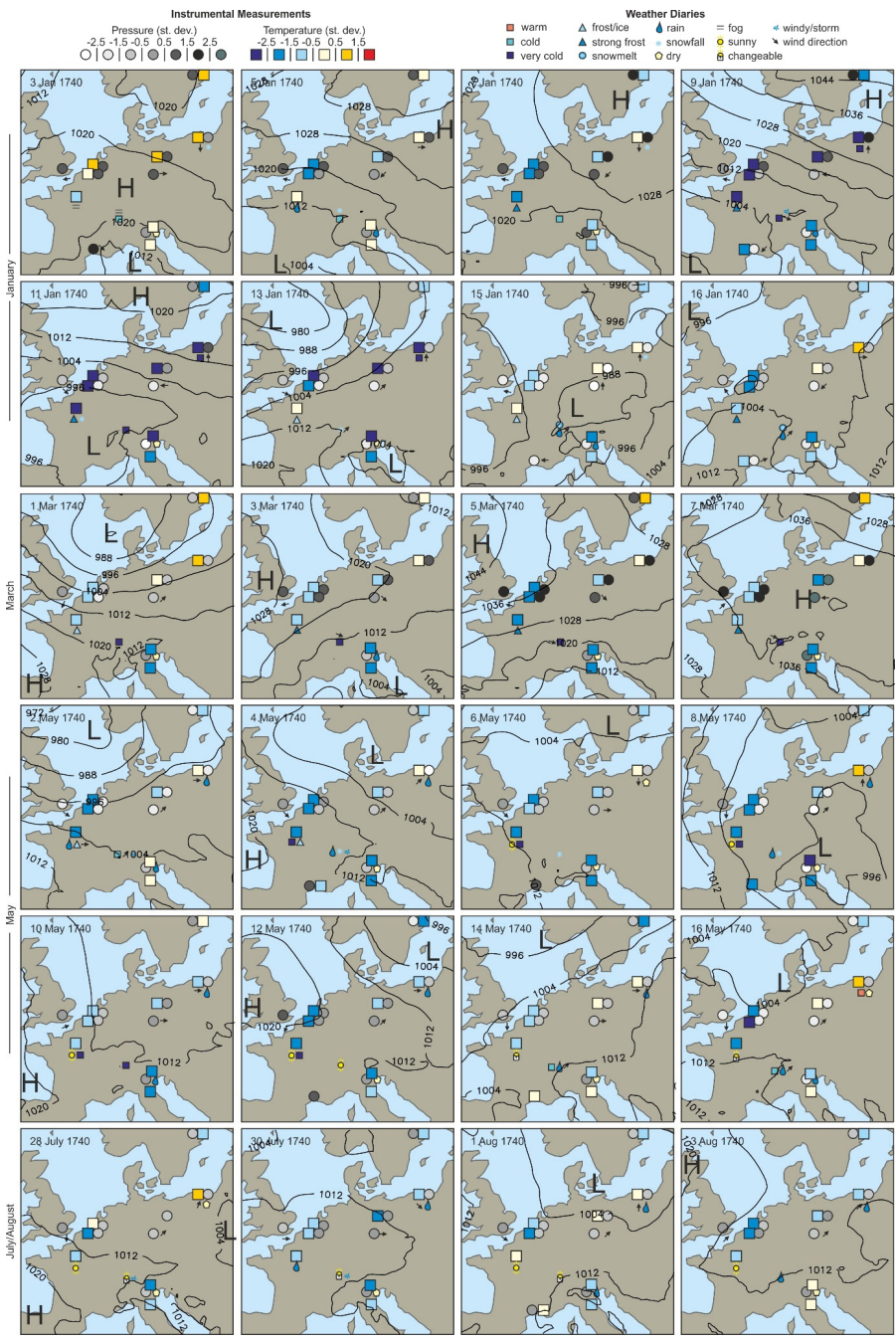
254 Plotting the daily data on a map, along with the weather observations and the analog pressure
 255 reconstructions allows an inspection of the pressure systems and of the flow over central Europe.
 256 During the cold spell in January (Fig. 4, top), a strong high-pressure system established over
 257 Scandinavia, and at the same time a rather strong low pressure system developed over the northern
 258 Mediterranean, causing a strong inverse pressure gradient across Europe. This situation can firmly be
 259 addressed as a Scandinavian blocking event, allowing cold, continental air to flow in from the east.
 260 The main spell lasted only five days, but further similarly extreme cold spells occurred in January and
 261 February. In the latter cases, positive pressure anomalies were strongest over London, but stretching
 262 into Scandinavia (not shown). Note that the sea-level pressure maps are based only on pressure
 263 observations and are independent of temperature and wind observations.

264 In the first half of March, pressure was high everywhere and temperatures were below normal
 265 everywhere except at Uppsala. Figure 4 depicts the beginning of this high-pressure period. After a
 266 strong low-pressure situation, pressure began to build up in the West (UK) and then established over
 267 the continent. The strongest pressure anomalies were observed first in Gdansk and Berlin. Again,
 268 continental Europe was in an easterly flow, bringing relatively (though not extremely) cold
 269 continental air to Central and Western Europe.

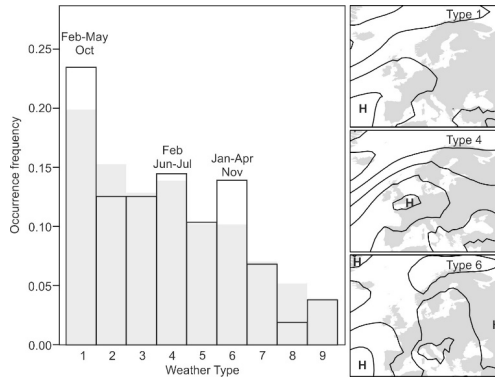
270 The generally low temperatures in 1740 not only included sharp but temporally limited drops of
 271 temperature due to cold spells, but also longer, persistent phases of below normal temperature. An

272 example is the third selected period in May 1740. During this period, pressure was relatively low over
273 continental Europe and arguably higher over England. The monthly mean reconstruction shows a
274 strong East Atlantic pattern throughout spring. Frequent westerly or northwesterly wind arguably
275 brought cold air from the northern North Atlantic, which at that time of the year is very cold relative
276 to the land. Finally, the lowest row in Fig. 4 shows a situation in late July and early August. It was
277 rather cold and rainy, with typical cyclonic weather dominating. The fifth period noted in Fig. 2 is the
278 month of October, which was persistently cold at most stations. [For reasons of length, the period and](#)
279 [which will be](#) analysed in the following based on monthly charts [rather than daily](#).

280



282 **Fig. 4.** Standardized anomalies of pressure and temperature as well as weather observations at stations and
283 analog sea-level pressure reconstruction (hPa) for four selected periods in Jan, Mar, May, and Jul/Aug 1740.



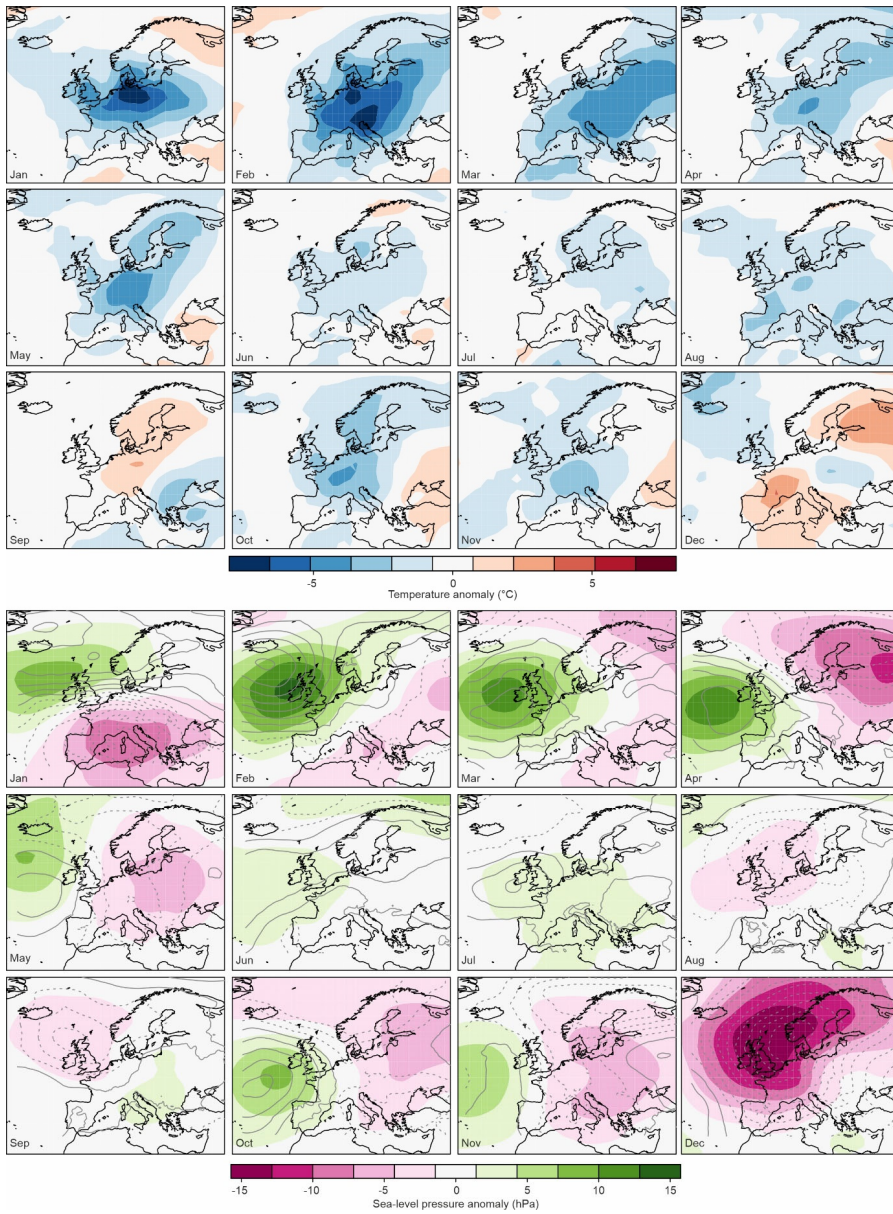
284 **Fig. 5.** Frequency of daily weather types in the CAP9 classification in 1740 (open rectangles) and in the period
285 1991-2020 (grey). Right insets show the composite fields for sea-level pressure for types 1, 4, and 6,
286 respectively, in 1940-2020 from ERA5.
287

288 Before focusing on monthly charts, though, we would like to analyse how the daily sea-level pressure
289 maps translate into monthly means. For this we analysed the frequency of daily weather types over
290 central Europe, specifically the CAP9 (Cluster Analysis of Principal Components with 9 types)
291 classification that reaches back to 1728 (Pfister et al., 2024). Three weather types were clearly
292 overrepresented in that year, namely 1, 6, and to a lesser extent 4. These patterns (displayed in Fig. 5,
293 right) are mostly types with high pressure systems over Western Europe.

294 We now turn to the analysis of monthly anomaly fields in the ModE-RA data sets (Fig. 6, see Fig. S2
295 for monthly anomaly fields from Oct-Dec 1739) and specifically the fields for October. Temperature
296 anomalies in this month were negative in Central Europe. Although they were not as strong as during
297 the winter months January to March, they reached down to -4°C which is remarkable for this time of
298 the year. As noted earlier, severe frost was observed in Versailles such that the grapes froze.

299 In ModE-RA we can also analyse monthly anomaly fields of sea-level pressure (Fig. 6, bottom, fields
300 for Oct-Dec 1739 are shown in Fig. S2). From January into June and then again in October and
301 November we find positive sea-level pressure anomalies in the East Atlantic and negative over
302 Eastern Europe. This is similar to the East Atlantic Pattern, which we will address in the following.
303 The positive anomalies could point to more frequent blocking situations. In Fig. 4 (top) we have
304 addressed Scandinavian blocking for the cold spell in January. However, this is not seen in the
305 monthly average, where the core of the positive anomaly is situated further in the West. The pattern
306 resemble more a negative North Atlantic Oscillation index, although the anomaly centres are shifted
307 southeastward.

308

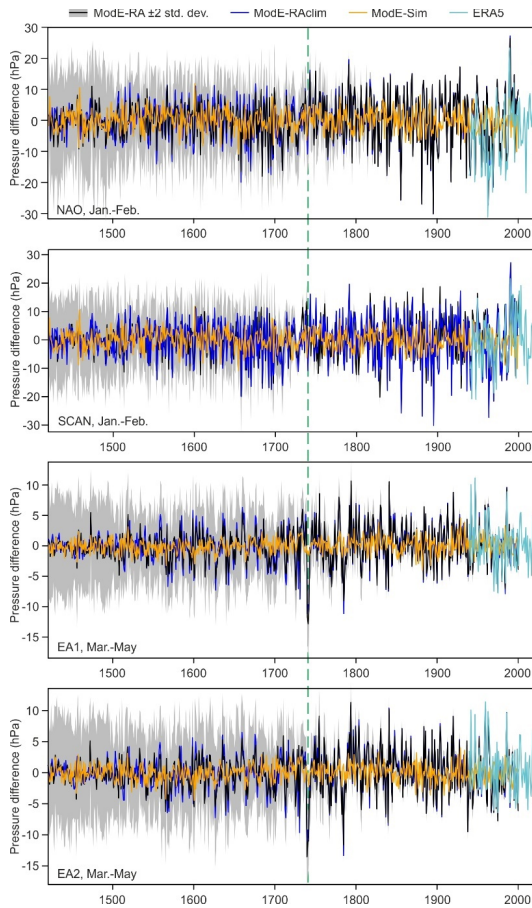


309

310 **Fig. 6.** Monthly anomalies (with respect to 1710-39) of (top) temperature and (bottom) sea-level pressure in
 311 1740 in the ModE-RA ensemble mean. The bottom figure also shows sea-level pressure anomalies from the
 312 analog approach (relative to 1991-2020, contour distance 2 hPa centred around zero, negative dashed).

313 We calculated indices for the NAO [and SCAN](#) for January and February and for the East Atlantic
 314 pattern for March to May for all three ModE products (Fig. 7, the ensemble spread is only shown for

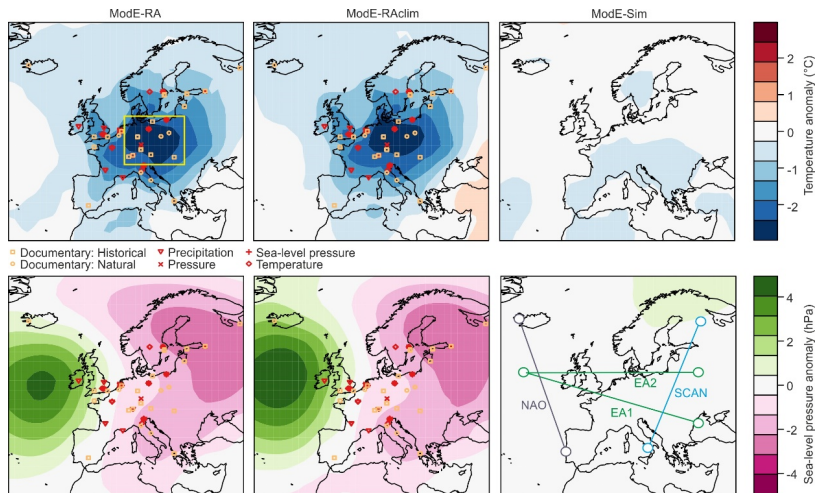
315 the ModE-RA for better visualisation). In ModE-RA and ModE-RAclim, which are very similar, the
316 NAO was negative in 1740, but it was by no means an extreme year. [Likewise, the SCAN index is](#)
317 [negative but not extreme.](#) However, the negative East Atlantic pattern in spring is unique in the entire
318 record since 1421, both for EA1 and EA2 (very similar results are found in the annual mean). The
319 analysis of ModE-Sim shows that only a small part of the variability is reproduced purely from the
320 model boundary conditions, which means that presumably the forced component of the signal is
321 relatively small at least in ModE-Sim. In order to extend the series to the present we also calculated
322 the indices in ERA5 (using 1991-2020 as a reference, correlations in the overlapping period for NAO,
323 EA1, and EA2 are 0.992, 0.936, 0.949, respectively). Neither of the series shows a trend, neither in
324 ModE-RA nor in ERA5. Also, no clear change in variability is seen in ModE-RA, although the recent
325 variability in the NAO in ERA5 is very large in a 600 year context.



326

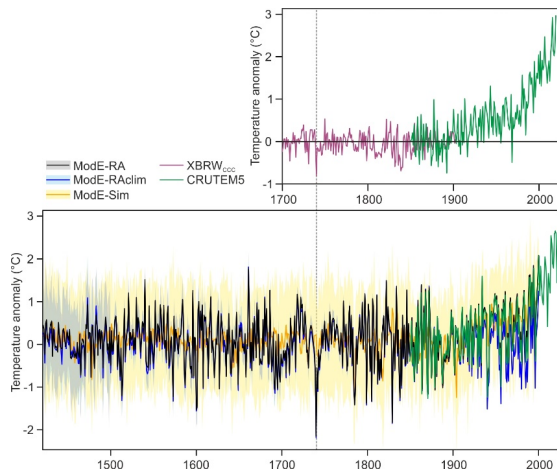
327 **Fig. 7.** Indices of the NAO [Index and SCAN](#) in Jan-Feb and of the EA1 and EA2 in Mar-May relative to 1710-
 328 39. Shown are the three data sets ModE-RA (grey shading denotes ± 2 standard deviations of the ensemble),
 329 ModE-RAclim and ModE-Sim as well as ERA5. The green dashed line marks the year 1740.

330 An interesting aspect in the monthly analysis is the persistence even at a seasonal and longer time
 331 scale. In particular, the East Atlantic pattern is persistent or recurring. We therefore also analysed the
 332 annual mean fields of temperature and pressure anomalies (Fig. 8). Again, ModE-RA and ModE-
 333 RAclim show very similar patterns. For temperature, the ModE-Sim shows negative temperature
 334 anomalies of up to $0.5\text{ }^{\circ}\text{C}$ over parts of Europe, hence there is a contribution of boundary conditions
 335 on a large scale, though much weaker than the full reconstruction. For sea-level pressure, there is no
 336 contribution from ModE-Sim. The pattern in the annual mean sea-level pressure anomaly is more
 337 similar to the East Atlantic pattern of Wallace and Gutzler (1981) rather than the corresponding
 338 pattern in Barneston and Livezey (1987).



339
 340 **Fig. 8.** Annual mean anomalies of (top) temperature and (bottom) sea-level pressure in 1740 in (left) ModE-RA,
 341 (middle) ModE-RAclim, and (right) ModE-Sim. Also shown are the location and types of observations for Oct
 342 1739-Mar 1740 on which ModE-RA and ModE-RAclim are based. The yellow rectangle (top left) shows the
 343 region defined as Central Europe. The bottom right figure shows the definition of NAO, [EA](#) and [SCAN](#)
 344 indices.

345



346
 347 **Fig. 9.** Top: Time series of cold season (May-Oct) mean temperature over northern extratropical (35-
 348 70° N) land areas (XBRW_{CC}). Bottom: Time series of annual mean Central European temperature in the three
 349 reconstructions ModE-RA, ModE-RAclim, and ModE-Sim. Shadings indicate two standard deviations of the
 350 ensemble.

351 To analyse how cold the year 1740 really was, we calculated Central European mean temperature in
 352 the three data sets. In fact, in ModE-RA, 1740 is the coldest year on record back to 1421 (outside the
 353 lower confidence interval of ModE-RA of any year), followed by 1829/30 (Fig. 9). The coldest 12-
 354 month period (not shown) is November 1739 to October 1740. The annual mean temperature of 1740
 355 was 2.15 °C below the preindustrial mean (1851-1900). Also shown are CRUTEM5 data in order to
 356 extend the climate reconstructions into the present. These data show a warming of 2.5 °C since the
 357 preindustrial, such that the cold year 1740 was more than 4 °C cooler than presently.

358
 359 *A large-scale view*

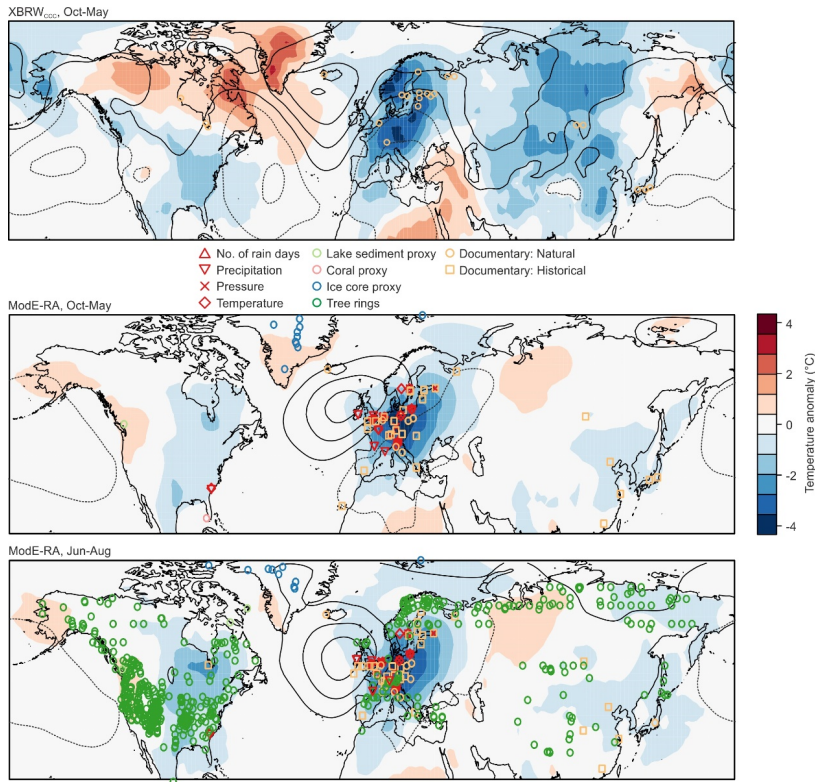
360 The winter of 1739/40 was not only cold in Europe, but also over North America and Eurasia. This
 361 can be seen in a recent reconstruction of cold-season (Oct-May) temperature based only on
 362 phenological data (Fig. 10). In fact, 1739/40 was the coldest cold season in the land-area averaged
 363 temperature between 35 and 70° N in this reconstruction (which reaches back to 1701, Reichen et al.
 364 2022, see Fig. 9, top). The low temperatures in North America are confirmed by a temperature series
 365 from Charleston (Fig. 2 Fig. S3) that was not included in the reconstruction shown in Fig. 10. In fact,
 366 this is also confirmed with documentary data. In North America, the summer of 1740 was cool and
 367 wet (Perly, 1891). However, in ModE-RA Siberia is warmer than in XBRW_{CC}.

368 Documentary data from China show that spring 1740 was late, both in Northern China and in
 369 Southern China, with the end date of snow being around 20 days later than average in Beijing-
 370 Zhangjiakou region and Nanjing (Xu, 2018; Gong et al., 1983). However, although narrative evidence

Formatted: Subscript

371 shows that the winter, especially the late winter, may have been colder than average in southern China
 372 (Ding and Zheng, 2017; Zhang, 2004), it was not an extremely cold winter based on existing
 373 reconstructions of East Asia (Hao et al., 2018; Wang et al., 2023).

374 The summer (Jun-Aug) temperature anomaly fields are very similar to those of the cold season (Fig.
 375 10). One reason might be that for some of the rivers, the thawing takes place only shortly after the
 376 start of the warm season assimilation window and these proxies are assimilated both for the cold and
 377 warm season. Likewise, since the warm season assimilation window covers Apr-Sep, the tree ring
 378 proxies in ModE-RA also affect the Oct-May period. However, the persistence might also be real as it
 379 also appears in the analog reconstructions (contours in Fig. 6). Similar as for the cold season, Siberia
 380 has also positive temperature anomalies in summer (arguably due to tree rings) such that the annual
 381 mean of 1740 was not the coldest year on record in global mean temperature in ModE-RA. Sea-level
 382 pressure anomalies show the clear EA pattern over Europe. In addition, they show a positive phase of
 383 the Pacific North-American (PNA) pattern, most pronounced in XBRW_{CCC}.



384
 385 **Fig. 10.** Anomalies of temperature and sea-level pressure (contour distance 2 hPa centred around zero, negative
 386 dashed) for (top) the cold season (Oct-May) 1739/40 in the XBRW_{CCC} data set (Reichen et al., 2022), (middle)
 387 the cold season 1739/40 in ModE-RA, and (bottom) summer (Jun-Aug) in ModE-RA, expressed as anomalies

388 from the preceding 30 years. For XBRW_{CCC}, which is based only on phenological data, orange circles mark the
389 locations (displayed with a slight offset if several observations, e.g., freezing and thawing dates, are available
390 from the same location). For ModE-RA, observations entering the data set are also shown.

391

392 *Role of forcings*

393 Finally, we analysed the role of oceanic influences (i.e., NINO3.4 in our case) and of external forcing
394 due to volcanic eruptions. ModE-RA, which is based on the monthly sea-surface temperature
395 reconstructions by Samakinwa et al. (2020), which in turn are based ~~on~~ annual reconstructions by
396 Neukom et al. (2019), show El Niño conditions in 1739 and partly in 1740. To analyse the possible
397 role of El Niño, we performed a correlation analyses, restricting our analysis to the years 1710-2000
398 because of the deteriorating quality further back. Results (Fig. ~~S3S4~~) show that almost all correlations
399 for all ensemble members for all indices (NAO in Jan-Feb, EA1 and EA2 in Mar-May) are within
400 ± 0.1 . The strongest (negative) correlations are found for the NAO. The box plots show the spread
401 among the ensemble members, which should not be confounded with the significance of the
402 correlations themselves. In fact, none of the correlations is statistically significant at $p = 0.05$.

403 Another influence could have come from the volcanic eruption of Mount Tarumae, 19-31 Aug 1739.
404 In the volcanic forcing data sets used in ModE-RA as well as in Sigl et al. (2015), this is not a very
405 big eruption, but with a global forcing of -2.4 W m^{-2} exceeds the threshold set in the methods section.
406 We analysed all eruptions with a global forcing stronger than -2 W m^{-2} , again restricting ourselves to
407 the time period 1710-2000 (Fig. S3). We find only weak effects of ~~the strong~~ eruptions on circulation,
408 such as a slightly positive response of the NAO in Jan-Feb and positive responses of the EA1 and
409 EA2 pattern.

410

411 **Discussion**

412 *Agreement between data sets and sequence of events*

413 The data sets (ModE-RA and XBRW_{CCC}, but also ModE-RA and the analog reconstruction) agree
414 well with each other, demonstrating that the extremely simple analog approach is suitable for the
415 purpose and that it is possible to study not only climate but also the weather of 1740. Moreover, the
416 findings from the reconstructions are well in line with the documentary evidence.

417 1740 was the coldest year in central Europe since 1421 and the coldest 12-month period was Nov
418 1739 to Oct 1740. The cause for the cold was a specific sequence of events. It started with
419 Scandinavian blocking, which brought cold continental air to Central Europe. Jones and Briffa (2006)
420 address Jan 1740 as a continental high-pressure situation. In our data, this concerns clearly the period
421 5-11 January, while the monthly mean of January as a whole does not show the strongest anomalies
422 over Scandinavia but rather over the UK/British Isles.

423 During spring (and actually most of the year) the dominant circulation pattern consisted of high
424 pressure or even blocking over the British Isles. This brought cold air from the northern North
425 Atlantic (which at that time of the year is much colder than the European continent) to central Europe.
426 August, then featured cyclonic weather, which brought cold and wet air masses from the West.

427 It is also important to note that the cold began already in autumn 1739 (Fig. S2) and that the following
428 two winters (most notably 1741-42) were also cold. Hence, a multiyear cold period followed a rather
429 mild decade, as pointed out by Jones and Briffa (2006).

430 *Dynamical aspects*

431 The year 1740 started with a negative NAO pattern, which however was not extreme. The cold air
432 outbreak in Jan 1740 is particularly noteworthy as temperature anomalies reached -6 standard
433 deviations. Was this the imprint of a sudden stratospheric warming (SSW)? Obviously, we have no
434 evidence and not even clear indications. SSWs are associated to a collapse of the polar vortex and can
435 affect surface weather for 30-60 days. More frequent cold air outbreaks in Northern Europe are a
436 possible consequence. It is not uncommon that SSWs are preceded by a pressure dipole over Europe
437 (Butler et al., 2017), to which Dec. 1739 bears some resemblance. Everything beyond that, however,
438 would be pure speculation.

439 Following this event, the circulation pattern over Europe took the form of a negative East Atlantic
440 pattern (EA1 or EA2) for a big part of the rest of the year. A similar pattern was also noted for spring
441 by Engel et al. (2013). In ModE-RA, the EA indices in Mar-May reached their most negative state on
442 record and similar for annual means. An existing reconstruction of the NAO and EA in winter
443 (Mellado-Cano et al., 2019), which is however based on only one series, also shows negative
444 anomalies in the winter 1739/40 in both indices.

445 In the Pacific North American sector, we find an anomaly pattern of sea-level pressure that resembles
446 a positive PNA phase. The relatively simple XBRW_{CCC} reconstruction shows this most clearly, but it
447 is also seen in the ModE-RA products.

448 *Comparison with other cold winters*

449 Although 1740 was unique as an entire year, the winter 1739/40 can be compared with other notable
450 winters. Many of the original written sources compare the winter with that of 1708/09. The lagoon of
451 Venice was also frozen in that year (Camuffo, 1987). The long reconstructed Dutch temperature series
452 (van Engelen et al., 2001; documentary before 1706 and instrumental afterwards) classifies 1739/40
453 with a severity of 8, which is also assigned to the winter of 1708/09, whereas 1683/84 1788/89 and
454 1829/30 are assessed as 9 (note that for 1788/89, daily reconstructions of preaaure and tempertaure
455 fields over Europe are also available, see Pappert et al., 2022). In the Central England Temperature
456 1683/84 ranks coldest, followed by 1739/40. More detailed comparisons of cold spells in 18th and
457 20th century winters are given in Pappert et al. (2022).

458

459 *Role of external forcings*

460 The role of boundary conditions (sea-surface temperatures, land surface) and external forcings can be
461 addressed using ModE-Sim. It shows a cooling in Central Europe of ca. 0.5 °C, i.e., a fraction of the
462 cooling could be due to boundary conditions. In terms of atmospheric circulation, we find a slight
463 negative NAO response in late winter and a very slightly negative EA pattern, but only a small part of
464 the deviations can be explained in that way.

465 In terms of external forcings, the arguably most likely candidate is the eruption of Mount Tarumae,
466 19-31 Aug 1739, which is incorporated in ModE-Sim. This was a highly explosive eruption (VEI=5),
467 but in terms of radiative forcing it was arguably not a very big eruption. It cannot be ruled out that the
468 eruption in the real world was larger, but there is no evidence. It can be stated that Aug 1740 was
469 typical for a volcanic summer, but given the location of Mount Tarumae (Hokkaido, Japan) it is not
470 clear whether an effect is still expected after one year. Analyses of NAO and EA indices with respect
471 to volcanic eruptions in general show only weak effects, which are of opposite sign to what was
472 observed in 1740. We therefore have no indication that the circulation anomalies in 1740 could have
473 been related to a volcanic eruption. Also, solar activity was average in 1740 in the PMIP4 forcings
474 (Jungclaus et al., 2017).

475 *Role of ocean and land surface*

476 In the reconstructions underlying ModE-Sim, 1739/40 were El Niño years. In order to study the
477 possible effect of El Niño on European climate, we performed a simple correlation approach in which
478 we correlated NINO3.4 with indices of NAO, EA1 and EA2. We find slightly negative correlations
479 with NAO in Jan-Feb, which although insignificant, indicate a possible influence. In contrast, for EA1
480 and EA2 in Mar-May we find very small, positive correlations.

481 The reconstructions for 1739/40 are consistent with an El Niño winter. For instance, we see the
482 expected positive PNA response in the cold season 1739/40. Also the negative NAO in Jan-Feb
483 agrees with the correlation analysis and with the literature. El Niño events can lead to a negative,
484 NAO-like response (Brönnimann, 2007), to a weak stratospheric polar vortex and to more frequent
485 SSWs (Domeisen et al., 2019). However, other aspects do not agree. For instance, for the EA1 and
486 EA2 indices we find a positive correlation with NINO3.4 but strongly negative anomalies in 1740.
487 Furthermore, the uncertainty of El Niño reconstructions 300 years ago is high. The reconstruction by
488 Li et al. (2013), for instance, has no clear El Niño event. [For the Atlantic Multidecadal Oscillation,
489 another possible influencing factor, we do not have good reconstructions to allow a more detailed
490 analysis. However, other studies have analysed effects on daily weather regimes \(Zampieri et al.,
491 2017\).](#)

492 Other teleconnection mechanisms leading to SSWs and subsequent cold air outbreaks in Europe have
493 been suggested in relation to recent Arctic sea ice decline. The proposed mechanism (Cohen et al.,
494 2014) involves an increase in snow cover over Eurasia in fall due to the low sea ice and increased
495 moisture transport. This could then amplify the planetary wave and lead to a collapse of the
496 stratospheric polar vortex. In order to test the plausibility of such a mechanism in this case we would
497 need to have information on sea ice or snow, which is very scattered for this period. A reconstruction
498 of autumn Barents-Kara Sea ice based on proxies (Zhang et al., 2018) indeed shows relatively low sea
499 ice values (compared to the 100 years before and after) around 1740. Indications for slightly cooler
500 and snowy conditions are also found from other records, but they were by no means extreme (see also
501 Reichen et al., 2022).

502 In existing reconstructions, the winter 1739/40 was colder than long-term average only in South
503 China, and in the Yangtze River region, it was colder than the past decades but not a cold winter in
504 past centuries (Hao et al., 2018; Hao et al., 2012). However, some of these reconstructions also
505 confirm an even colder winter in East Asia in 1741/42 and 1742/43. Also, the winter 1740/41 was
506 recognized as an extremely cold winter in southern China although not the coldest one based on
507 narrative records (Zheng et al., 2012). Snow cover might have provided a mechanism for the
508 persistence of anomalies over multiple winters (Reichen et al., 2022). However, again, this
509 mechanism remains speculative.

510 *Role of atmospheric internal variability*

511 Finally, we have to address the role of internal atmospheric variability. In our view, after having
512 studied possible forcing factors and after having found no clear indications for external forcings,
513 oceanic or land surface effects, we ascribe most of the anomalous circulation to internal variability (in
514 line with interpretations by Engler et al., 2013, and Jones and Briffa, 2006). Specifically, the record
515 low EA1 and EA2 indices cannot be explained by any of the suggested mechanisms. These were
516 however, dominating the cold of the year 1740.

517 **Conclusions**

518 The year 1740 was arguably the coldest in Central Europe since 1421. The annual mean temperature
519 was 2 °C below pre-industrial levels, and the extended cold season 1739/40 was also the coldest one
520 for the northern midlatitude land mass since 1700. The winter of 1739/40 and the cold year of 1740
521 had severe consequences for societies in Europe, including increased prices and famine. It is therefore
522 relevant to assess the chain of processes causing such a cold year. Still even this large excursion of
523 climate dwarfs against changes observed in the last 120 years.

524 The analysis revealed that the coldness was due to the special sequence of events, i.e., a continental
525 high/Scandinavian blocking in January, then negative East Atlantic pattern during spring, a cyclonic
526 summer, and again negative EA pattern. Most of this is arguably due to internal atmospheric

527 variability. We studied many possible forcings and system effects and found no clear indications for a
528 forced signal. Only the circulation anomalies in January might have been made more likely by a
529 possible El Niño event, or, even much more speculative, low Arctic sea ice and increased snow cover.
530 Furthermore, part of the general cooling over Europe can be explained by a volcanic eruption in 1739.
531 However, this explains only a small fraction, and the most outstanding feature of this climatic
532 anomaly, the negative East Atlantic pattern that persisted for almost a year, shows no indication of a
533 forced contribution.

534 The analysis shows that extreme internal variability of the atmosphere is possible. It also shows that
535 daily weather data and a new monthly climate reconstruction together allow a detailed insight into the
536 mechanisms that brought forth a momentous climate event that happened close to 300 years back in
537 the past.

538

539 **Data availability statement:** The ModE-RA, ModE-RAclim, and ModE-Sim data (Valler et al., 2024) can be
540 downloaded from DKRZ (<https://www.wdc-climate.de/ui/entry?acronym=ModE-RA>). ERA5 reanalysis data are
541 available from the Copernicus Climate Change Service Data Store. XBRW_{CCC} data are available from
542 PANGAEA (Reichen et al., 2022, <https://doi.pangaea.de/10.1594/PANGAEA.934288>), CRUTEM5 is available
543 from <https://crudata.uea.ac.uk/cru/data/temperature/> (accessed 4 Mar 2024). The historical station data are
544 available from figshare (doi:10.6084/m9.figshare.25879186). The St. Blaise data were taken from EURO-
545 CLIMHIST (Pfister et al., 2017, <https://www.euroclimhist.unibe.ch/>, accessed 4 Mar 2024).

546 **Code availability statement:** All analyses were done in R using standard code. The ModE-RA family of
547 products can be accessed through and all corresponding analyses can also be done at the website: <https://mode->
548 [ra.unibe.ch/climeapp/](https://mode-ra.unibe.ch/climeapp/).

549 **Author contributions:** SB performed the analyses, JF and SC provided historical observations and
550 documentary sources, LP provided the weather type reconstructions. All authors contributed to writing the
551 paper.

552 **Funding Information:** The work was funded by the Swiss National Science Foundation projects WeaR
553 (188701) and DVDW (219746) and the European Commission through H2020 (ERC Grant PALAEO-RA
554 787574) and the National Science Centre, Poland project No. 2020/37/B/ST10/00710.

555 **Competing interests.** The contact author has declared that none of the authors has any competing interests.

556 **Acknowledgements.** We would like to thank Yuri Brugnara, Dario Camuffo, Daniel Rousseau, Richard Cornes,
557 and Rolando Garcia-Herrera for providing the pressure and wind data. The simulations underlying ModE-RA
558 were performed at the Swiss Supercomputer Centre (CSCS).

559 **References**

- 560 Barnston, A. G., and Livezey, R. E.: Classification, Seasonality and Persistence of Low-Frequency Atmospheric
561 Circulation Patterns. *Mon. Wea. Rev.*, 115, 1083–1126, 1987.
- 562 Barriopedro, D., Gallego, D., Álvarez-Castro, M. C., García-Herrera, R., Wheeler, D., Peña-Ortiz, C., and
563 Barbosa, S. M.: Witnessing North Atlantic westerlies variability from ships' logbooks (1685-2008). *Clim.*
564 *Dyn.*, 43, 939-955, 2014.
- 565 Bergström, H. and Moberg, A.: Daily air temperature and pressure series for Uppsala (1722–1998). *Clim.*
566 *Change*, 53, 213–252, 2002.
- 567 Brönnimann, S.: Impact of El Niño–Southern Oscillation on European climate. *Rev. Geophys.*, 45, RG3003,
568 2007.
- 569 Brönnimann, S. Allan, R., Ashcroft, L., Baer, S., Barriendos, M., Brázdil, R., Brugnara, Y., Brunet, M.,
570 Brunetti, M., Chimani, B., Cornes, R., Domínguez-Castro, F., Filipiak, J., Founda, D., García Herrera, R.,
571 Gergis, J., Grab, S., Hannak, L., Huhtamaa, H., Jacobsen, K. S., Jones, P., Jourdain, S., Kiss, A., Lin, K. E.,
572 Lorrey, A., Lundstad, E., Luterbacher, J., Mauelshagen, F., Maugeri, M., Maughan, N., Moberg, A., Neukom,
573 R., Nicholson, S., Noone, S., Nordli, Ø., Ólafsdóttir, K. B., Pearce, P. R., Pfister, L., Pribyl, K., Przybylak, R.,
574 Pudmenzky, C., Rasol, D., Reichenbach, D., Řezníčková, L., Rodrigo, F. S., Rohde, R., Rohr, C., Skrynyk,
575 O., Slonosky, V., Thorne, P., Valente, M. A., Vaquero, J. M., Westcott, N. E., Williamson, F., and
576 Wyszynski, P.: Unlocking pre-1850 instrumental meteorological records: A global inventory, *B. Am.*
577 *Meteorol. Soc.*, 100, ES389–ES413, 2019.
- 578 Brönnimann, S. and Brugnara, Y.: The weather diaries of the Kirch family: Leipzig, Guben, and Berlin, 1677-
579 1774. *Clim. Past*, 19, 1435–1445, <https://doi.org/10.5194/cp-19-1435-2023>, 2023.
- 580 Butler, A. H., Sjöberg, J. P., Seidel, D. J., and Rosenlof, K. H.: A sudden stratospheric warming compendium,
581 *Earth Syst. Sci. Data*, 9, 63–76, <https://doi.org/10.5194/essd-9-63-2017>, 2017.
- 582 [Camuffo D.: Freezing of the venetian lagoon since the 9th century a.d. in comparison to the climate of western](#)
583 [Europe and England, *Climatic Change* 10, 43-66, 1987.](#)
- 584 Camuffo, D., and Jones, P.: Improved understanding of past climatic variability from early daily European
585 instrumental sources. *Climatic Change*, 53, 1–4, 2002, <https://doi.org/10.1023/A:1014902904197>
- 586 [Camuffo D., della Valle, A., Bertolin, C. and Santorelli, E.: Temperature observations in Bologna, Italy, from](#)
587 [1715 to 1815: a comparison with other contemporary series and an overview of three centuries of changing](#)
588 [climate. *Climatic Change*, 142, 7-22. DOI 10.1007/s10584-017-1931-2](#), 2017
- 589 Cohen, J., Screen, J., Furtado, J., Barlow, M., Whittleston, D., Coumou, D., Francis, J., Dethloff, K., Entekhabi,
590 D., Overland, J., and Jones, J.: Recent Arctic amplification and extreme mid-latitude weather. *Nature Geosci.*,
591 7, 627–637, 2014, <https://doi.org/10.1038/ngeo2234>
- 592 Cornes R. C., Jones, P. D., Briffa, K. R., and Osborn, T. J.: A daily series of mean sea-level pressure for
593 London, 1692-2007. *Int. J. Climatol.*, 32, 641–656, 2012.
- 594 Cornes, R. C., Jones, P. D., Brandsma, T., Cendrier, D., and Jourdain, S. (2023) The London, Paris and De Bilt
595 sub-daily pressure series. *Geoscience Data Journal*, 00, 1–12. Available from:
596 <https://doi.org/10.1002/gdj3.226>
- 597 Dickson, D.: *Arctic Ireland: The Extraordinary Story of the Great Frost and Forgotten Famine of 1740–1741*,
598 Whiterow Press, Belfast, 1997.
- 599 Ding, L. and Zheng, J.: Reconstruction and characteristics of series of winter cold index in South China in the
600 past 300 years. *Geographical Research*, 36, 1183-1189, <https://doi.org/10.11821/dlyj201706015>, 2017.
- 601 Domeisen, D. I., Garfinkel, C. I., and Butler, A. H.: The teleconnection of El Niño Southern Oscillation to the
602 stratosphere. *Rev. Geophys.*, 57, 5–47, <https://doi.org/10.1029/2018RG000596>, 2019.
- 603 Engler, S., Mauelshagen, F., Werner, J., and Luterbacher, J.: The Irish famine of 1740–1741: famine
604 vulnerability and "climate migration", *Clim. Past*, 9, 1161–1179, <https://doi.org/10.5194/cp-9-1161-2013>,
605 2013.

Formatted: Font: 10 pt

606 Filipiak, J., Przybylak, R., and Oliński, P.: The longest one-man weather chronicle (1721–1786) by Gottfried
607 Reyger for Gdańsk, Poland as a source for improved understanding of past climate variability. *Int. J.*
608 *Climatol.*, 39, 828–842, doi: 10.1002/joc.5845, 2019.

609 Gillespie, T.: The great Irish frost of winter 1739–40 in Mayo recalled. *The Connaught Telegraph*, 30 December
610 1939 (<https://www.con-telegraph.ie/2022/12/31/the-great-irish-frost-of-winter-1739-40-in-mayo-recalled/>)

611 Gong, G., Zhang, P., and Zhang, J.: A study on the climate of the 18th century of the lower Changjiang valley in
612 China. *Geographical Research*, 2, 20–33, <https://doi.org/10.11821/yj1983020003>, 1983.

613 Hao, Z. X., Zheng, J. Y., Ge, Q. S. and Wang, W. C.: Winter temperature variations over the middle and lower
614 reaches of the Yangtze River since 1736 AD. *Clim. Past*, 8, 1023–1030, 2012.

615 Hao, Z., Yu, Y., Ge, Q. and Zheng, J.: Reconstruction of high-resolution climate data over China from rainfall
616 and snowfall records in the Qing Dynasty. *WIREs Clim Change*, 9, e517, 2018.

617 Hersbach, H., Bell, B., Berrisford, P., Hirahara, S., Horányi, A., Muñoz-Sabater, J., Nicolas, J., Peubey, C.,
618 Radu, R., Schepers, D., Simmons, A., Soci, C., Abdalla, S., Abellan, X., Balsamo, G., Bechtold, P., Biavati,
619 G., Bidlot, J., Bonavita, M., De Chiara, G., Dahlgren, P., Dee, D., Diamantakis, M., Dragani, R., Flemming,
620 J., Forbes, R., Fuentes, M., Geer, A., Haimberger, L., Healy, S., Hogan, R. J., Hólm, E., Janisková, M.,
621 Keeley, S., Laloyaux, P., Lopez, P., Lupu, C., Radnoti, G., de Rosnay, P., Rozum, I., Vamborg, F., Villaume,
622 S., and Thépaut, J.-N.: The ERA5 global reanalysis. *Q. J. R. Meteorol. Soc.*, 146, 1999–2049, 2020.
623 <https://doi.org/10.1002/qj.3803>

624 Jones, P. D., and Briffa, K.R.: Unusual Climate in Northwest Europe During the Period 1730 to 1745 Based on
625 Instrumental and Documentary Data. *Clim. Change* 79, 361–379 (2006). [https://doi.org/10.1007/s10584-006-](https://doi.org/10.1007/s10584-006-9078-6)
626 [9078-6](https://doi.org/10.1007/s10584-006-9078-6)

627 Jungclauss, J. H., Bard, E., Baroni, M., Braconnot, P., Cao, J., Chini, L. P., Egorova, T., Evans, M., González-
628 Rouco, J. F., Goosse, H., Hurrell, G. C., Joos, F., Kaplan, J. O., Khodri, M., Klein Goldewijk, K., Krivova, N.,
629 LeGrande, A. N., Lorenz, S. J., Luterbacher, J., Man, W., Maycock, A. C., Meinshausen, M., Moberg, A.,
630 Muscheler, R., Nehrbaas-Ahles, C., Otto-Bliesner, B. I., Phipps, S. J., Pongratz, J., Rozanov, E., Schmidt, G.
631 A., Schmidt, H., Schmutz, W., Schurer, A., Shapiro, A. I., Sigl, M., Smerdon, J. E., Solanki, S. K.,
632 Timmreck, C., Toohey, M., Usoskin, I. G., Wagner, S., Wu, C.-J., Yeo, K. L., Zanchettin, D., Zhang, Q., and
633 Zorita, E.: The PMIP4 contribution to CMIP6 – Part 3: The last millennium, scientific objective, and
634 experimental design for the PMIP4 past1000 simulations. *Geosci. Model Dev.*, 10, 4005–4033,
635 <https://doi.org/10.5194/gmd-10-4005-2017>, 2017.

636 Lamb, H. H. Britain's Changing Climate. *The Geographical Journal*, 133, 445–466,
637 <https://doi.org/10.2307/1794473>, 1967.

638 Li, J., Xie, S.-P., Cook, E. R., Morales, M. S., Christie, D. A., Johnson, N. C., Chen, F., D'Arrigo, R., Fowler, A.
639 M., Gou, X. and Fang, K.: El Niño modulations over the past seven centuries. *Nature Climate Change*, 3,
640 822–826, 10.1038/nclimate1936, 2013.

641 Lundstad, E., Brugnara, Y., Pappert, D., Kopp, J., Hürzeler, A., Andersson, A., Chimani, B., Cornes, R.,
642 Demarée, G., Filipiak, J., Gates, L., Ives, G. L., Jones, J. M., Jourdain, S., Kiss, A., Nicholson, S. E.,
643 Przybylak, R., Jones, P. D., Rousseau, D., Tinz, B., Rodrigo, F. S., Grab, S., Domínguez-Castro, F.,
644 Slonosky, V., Cooper, J., Brunet, N. and Brönnimann, S.: Global historical climate database - HCLIM.
645 *Scientific Data*, 10, 44, 2023.

646 Luterbacher, J., Xoplaki, E., Dietrich, D., Rickli, R., Jacobeit, J., Beck, C., Gyalistras, D., Schmutz, C., and
647 Wanner, H.: Reconstruction of Sea Level Pressure fields over the Eastern North Atlantic and Europe back to
648 1500. *Clim. Dynam.*, 18, 545–561, 2002.

649 Manley, G.: The Great Winter of 1740. *Weather* 14, 11–17, 1957.

650 [Manley, G.: Central England Temperatures: monthly means 1659 to 1973. *Q. J. R. Meteorol. Soc.*, 100, 389–405,
651 1974.](https://doi.org/10.1002/joc.3887)

652 [Mateus, C.: Searching for historical meteorological observations on the Island of Ireland. *Weather*, 76: 160–
653 165, 2021. <https://doi.org/10.1002/wea.3887>.](https://doi.org/10.1002/wea.3887)

Formatted: Font: (Default) Times New Roman, 10 pt

Formatted: Font: 10 pt

Formatted: Font: (Default) Times New Roman, 10 pt

Formatted: Font: 10 pt

Formatted: Font: (Default) Times New Roman, 10 pt

Formatted: Font: 10 pt

Formatted: Font: (Default) Times New Roman, 10 pt

Formatted: Font: 10 pt

Formatted: Font: (Default) Times New Roman, 10 pt

Formatted: Font: 10 pt

Formatted: Font: (Default) Times New Roman, 10 pt

Formatted: Font: 10 pt

Formatted: Font: (Default) Times New Roman, 10 pt

Formatted: Font: (Default) Times New Roman, 10 pt

Formatted: Font: (Default) Times New Roman, 10 pt

Formatted: Font: (Default) Times New Roman, 10 pt

654 Mellado-Cano, J., Barriopedro, D., García-Herrera, R., Trigo, R. M., and Hernández, A.: Examining the North
655 Atlantic Oscillation, East Atlantic Pattern, and Jet Variability since 1685. *J. Clim.*, 32, 6285–6298,
656 <https://doi.org/10.1175/JCLI-D-19-0135.1>, 2019.

657 Neukom, R., Steiger, N., Gómez-Navarro, J.J. Wang, J., Werner, J. P.: No evidence for globally coherent warm
658 and cold periods over the preindustrial Common Era. *Nature*, 571, 550–554, <https://doi.org/10.1038/s41586-019-1401-2>, 2019.

660 Osborn, T. J. et al. Land surface air temperature variations across the globe updated to 2019: the CRUTEM5
661 dataset. *J. Geophys. Res.* 126, e2019JD032352, 2021.

662 [Parker, D. E., Legg, T. P. and Folland, C. K.: A new daily Central England Temperature Series, 1772-1991. *Int. J. Clim.*, 12, 317-342, 1992.](#)

664 Pappert, D., Barriendos, M., Brugnara, Y., Imfeld, N., Jourdain, S., Przybylak, R., Rohr, C. and Brönnimann, S.:
665 Statistical reconstruction of daily temperature and sea-level pressure in Europe for the severe winter 1788/9.
666 *Clim. Past*, 18, 2545–2565, 2022.

667 Perley, S.: *Historic Storms of New England*. Salem Press Publishing and Printing Company, 1891.

668 Pfister C., and Wanner H.: *Climate and Society in Europe*. Bern: Haupt Verlag, 2021.

669 Pfister, C., Rohr, C., and Jover, A. C. C.: Euro-Climhist: eine Datenplattform der Universität Bern zur Witte-
670 rungs-, Klima- und Katastrophengeschichte. *Wasser Energie Luft*, 109, 45–48, 2017.

671 Pfister, L., Wilhelm, L., Brugnara, Y., Imfeld, N., Brönnimann, S.: Weathertype Reconstruction using Machine
672 Learning Approaches. *EGUsphere* [preprint], 2024, <https://doi.org/10.5194/egusphere-2024-1346>.

673 Post, J. D.: Climatic variability and the European mortality wave of the early 1740s, *J. Interdiscipl. Hist.*, 15, 1–
674 30, 1984.

675 Reichen, L., Burgdorf, A.-M., Brönnimann, S., Rutishauser, M., Franke, J., Valler, V., Samakinwa, E., Hand,
676 R., and Brugnara, Y.: A Decade of Cold Eurasian Winters Reconstructed for the Early 19th Century. *Nature*
677 *Communications*, 13, 2116, <https://doi.org/10.1038/s41467-022-29677-8>, 2022.

678 Rousseau, D.: Le cahier d'observations météorologiques de Réaumur. Ses mesures de températures de 1732 à
679 1757. *La Météorologie*, 105, 21-28, 2019.

680 Samakinwa, E., Valler, V., Hand, R., Neukom, R., Gómez-Navarro, J. J., Kennedy, J., Rayner, N. A. and
681 Brönnimann, S.: An ensemble reconstruction of global monthly sea surface temperature and sea ice
682 concentration 1000–1849. *Scientific Data*, 8, 261, 2021.

683 Sigl, M., Winstrup, M., McConnell, J. R., Welten, K. C., Plunkett, G., Ludlow, F., Büntgen, U., Caffee, M.,
684 Chellman, N., Dahl-Jensen, D., Fischer, H., Kipfstuhl, S., Kostick, C., Maselli, O. J., Mekhaldi, F.,
685 Mulvaney, R., Muscheler, R., Pasteris, D. R., Pilcher, J. R., Salzer, M., Schüpbach, S., Steffensen, J. P.,
686 Vinther, B. M., and Woodruff, T. E.: Timing and climate forcing of volcanic eruptions for the past 2,500
687 years. *Nature*, 523, 543-549, 2015.

688 Société Météorologique de France: *Annuaire de la Société Météorologique de France*, 14, 1866.

689 [Stefanini, C., Becherini, F., Valle, A.d., and Camuffo, D.: Homogenization of the Long Instrumental Daily-
690 Temperature Series in Padua, Italy \(1725–2023\). *Climate*, 12, 86, <https://doi.org/10.3390/cli12060086>, 2024.](#)

691 Titchner, H. A. and Rayner, N. A.: The Met Office Hadley Centre sea ice and sea surface temperature data set,
692 version 2: 1. Sea ice concentrations. *J. Geophys. Res.*, 119, 2864-2889, doi: 10.1002/2013JD020316, 2014.

693 [van Engelen, A. F. Buisman, V., J. and Ijnsen, F.: A millennium of weather, winds and water in the low
694 countries, in *History and Climate: Memories of the Future?*, edited by P. D. Jones et al., pp. 101–124,
695 Plenum, New York, 2001.](#)

696 Valler, V., Franke, J., Brugnara, Y., and Brönnimann, S.: An updated global atmospheric paleo-reanalysis
697 covering the last 400 years. *Geosc. Data J.*, 9, 89– 107, doi: 10.1002/gdj3.121, 2022.

698 Valler, V., Franke, J., Brugnara, Y., Samakinwa, E., Hand, R., Burgdorf, A.-M., Lipfert, L., Friedman, A.,
699 Lundstad, E., and Brönnimann, S.: ModE-RA - a global monthly paleo-reanalysis of the modern era (1421-
700 2008). *Scientific Data*. 11, 36, <https://doi.org/10.1038/s41597-023-02733-8>, 2024.

Field Code Changed

- 701 Wallace, J. M., and Gutzler, D. S: Teleconnections in the Geopotential Height Field during the Northern
702 Hemisphere Winter. *Mon. Wea. Rev.*, 109, 784–812, [https://doi.org/10.1175/1520-0493\(1981\)109<0784:TITGHF>2.0.CO;2](https://doi.org/10.1175/1520-0493(1981)109<0784:TITGHF>2.0.CO;2), 1981.
- 704 Wang, J., Yang, B., Wang, Z., Luterbacher, J. and Ljungqvist, F. C.: Recent weakening of seasonal temperature
705 difference in East Asia beyond the historical range of variability since the 14th century. *Sci. China Earth Sci.*,
706 66, 1133–1146, <https://doi.org/10.1007/s11430-022-1066-5>, 2023.
- 707 Xu, Q.: Analysis of temperature and snow characteristics in winter in Beijing and Zhangjiakou region, Master
708 thesis, Agronomy College, Shenyang Agricultural University, China, 2017.
- 709 [Zampieri, M., Toreti, A., Schindler, A., Scoccimarro, E. and Gualdi, S: Atlantic multi-decadal oscillation
710 influence on weather regimes over Europe and the Mediterranean in spring and summer". *Global and
711 Planetary Change*. 151, 92-100, 2017, doi:10.1016/j.gloplacha.2016.08.014.](#)
- 712 Zhang, D.: A compendium of Chinese meteorological records of the last 3,000 years. Phoenix House. Ltd.,
713 2013.
- 714 Zhang, Q., Xiao, C. D., Ding, M. H., and Dou T. F.: Reconstruction of autumn sea ice extent changes since
715 AD1289 in the Barents-Kara Sea, Arctic. *Science China Earth Sciences*, <https://doi.org/10.1007/s11430-017-9196-4>, 2018.
- 717 Zheng, J. Y., Ding, L. L., Hao, Z. X. and Ge, Q. S.: Extreme cold winter events in southern China during AD
718 1650–2000. *Boreas*, 41, 1–12, 2012.